U.S. DEPARTMENT OF THE INTERIOR

U.S. GEOLOGICAL SURVEY

Seismicity Patterns in Southern California Before and After the 1994 Northridge Earthquake: A Preliminary Report

by

Paul A. Reasenberg

Open-File Report 95-484

This report is preliminary and has not been reviewed for conformity with U.S. Geological Survey editorial standards. Any use of trade, product or firm names is for descriptive purposes only and does not imply endorsement by the U.S. Government.

1995

Menlo Park, CA 94025

INTRODUCTION

This report describes seismicity patterns in southern California before and after the January 17, 1994 Northridge (M_w = 6.7) earthquake. The report is preliminary in the sense that it was prepared as soon as the necessary data became available. The observations presented below of seismicity one year before and up to 3 months after the Northridge earthquake were compiled on April 18, 1994. The observations of the second quarter-year of post-seismic activity (April 17 to July 17) were compiled the week of July 18, 1994. The scope of the report is limited to the description of seismicity patterns, and excludes analysis of the regional geology, static and dynamic stresses and deformations associated with the Northridge (or previous) earthquakes, or other factors that may be relevant to a full understanding of the regional tectonics. For a summary of the Northridge earthquake see Scientists of the U.S. Geological Survey and the Southern California Earthquake Center (1994).

Various meanings have been ascribed to the term "pattern". Taken out of context, any "snapshot" or finite sample taken from nature will contain patterns. For example, a photograph of a snowflake, the set of today's winning lottery numbers, and a 3-month sample of earthquake occurrences each contains a particular pattern or structure. The hexagonal patterns in the snowflake are, of course, produced by the underlying molecular structure, which is why they accurately predict the symmetry in all other snowflakes. On the other hand, the lucky numbers from today's lottery contain no information about the process that created them that is predictive of tommorow's winning numbers (presumably). Earthquake occurrence lies somewhere between these

extremes. While crustal stress and strain, fluid pressure, temperature and other physical factors clearly play a role in the production of earthquakes, deterministic theory, such as that available for predicting the snowflake's hexagonal symmetry, is lacking for earthquake occurrence, largely due to geologic heterogeneity in the crust and nonlinear behavior of rocks at high pressures and temperatures. These factors introduce complexity (appearing as randomness) into both field and laboratory observations. So probably some of the patterns in seismicity contain predictive information and some are noise (in the sense that they are not useful for prediction), and the challange is to distinguish between the two.

When considered in this context, the interpretation of seismicity patterns is understood to be an inexact science. For example, while probabilistic estimates of earthquake occurrence based on unusual seismicity patterns have been made (Keilis-Borok et al., 1990; Healy et al., 1992), the probability gain they provide may be small and their accuracy hard to assess. Temporal patterns are elusive. Regional seismicity sometimes becomes quiescent before an earthquake and sometimes intensifies (Reasenberg and Matthews, 1988; Wiemer and Wyss, 1994; Sykes and Jaume, 1990). Spatial patterns, such as the ones shown below, are particularly inticing, especially when simple forms such as "donuts" or migrations appear, but guidelines for the sensible interpretation of these patterns are weak or absent because geologic, geodetic and other regional information needed to support them is often ambiguous or unavailable.

On the other hand, there is little doubt that some seismicity patterns contain information that can be understood and utilized. Perhaps the most obvious example is the

aftershock sequence (Utsu, 1971). Others include foreshock occurrence (Agnew and Jones, 1991) and the self-similar distribution of earthquake sizes, expressed as the Gutenberg-Richter relation (Richter, 1958). While the physical mechanisms underlying these basic and widely observed patterns are not fully understood, the empirical patterns themselves are repeatable, and thus support statistical models that provide probabilistic forecasts of earthquake activity (Reasenberg and Jones, 1989; Agnew and Jones, 1991; Reasenberg and Jones, 1994).

Some recent studies have shown clear agreement between static stress changes calculated with elastic dislocation models and the subsequent spatial and temporal distribution of earthquakes (King et al., 1994; Stein et al., 1992, 1994; Reasenberg and Simpson, 1992; Harris et al., 1995). These studies showed that the seismicity "signal" produced by sudden static stress changes is detectable in the "noise" of background seismicity, and that these stress changes, which can be estimated with simple models, contain predictive information about future earthquake occurrence. In the case of the Northridge earthquake, Stein et al. (1994) and Harris et al. (1995) showed correlative and apparently causal relationships between the stresses produced by the earthquake and the spatial and temporal distribution of seismicity in southern California after it, when reasonable models for regional faults and stresses were adopted. The success of these studies raises hope that future interpretations of seismicity patterns may be guided by increasingly well founded, predictive models. However, additional knowledge of existing faults, present deformation rates, crustal fluids and stresses are needed to support such models. It is hoped that the regional seismic observations surrounding the Northridge earthquake that are presented below may further stimulate

such developments. The suggestions in this report of possible spatial and temporal seismicity patterns are offered in an exploratory and tentative spirit. Whether these observations represent repeatable patterns or are essentially a unique snapshot of "noise" without predictive value for southern California (or any where else) remains to be seen. Continued hypothesis testing using data from additional earthquakes and more realistic models of the crust under southern California will be needed.

DATA AND METHODOLOGY

The study area in this report (defined as the region included in Figure 1) is approximately centered on the epicenter of the Northridge earthquake, and extends approximately 100 km in all directions from the earthquake (Figure 1). Earthquake data ($M \geq 1.0$) were taken from the Southern California Seismograph Network catalog (Wald, et al., 1994). Faults shown in Figure 1 are known active faults taken from Jennings (1992).

In Figures 2-5, 7-10 and 15-16, the color represents a change in average seismicity rate between a background period and a foreground period. The background period used in the calculation of rate changes in these figures is the 5.6-year period from July 1, 1987 to January 17, 1993. This was a fairly stable period in the catalog. Several foreground periods were used. They are the four quarter-year periods before the Northridge earthquake (Figures 2-5), the first quarter-year period after the Northridge earthquake (Figures 7-10), and the second quarter-year period after the Northridge earthquake (Figures 15-16). Spatial smoothing (using either a 5 km or 2 km radius gaussian smoothing kernel) was applied to the images and accounts for the smeared out colors surrounding individual earthquakes and clusters. Our method for representing the change in seismicity rate involves use of the statistic (Matthews and Reasenberg, 1988; Reasenberg and Matthews, 1988). The β statistic is defined as the difference between the actual number of earthquakes in the foreground period and the number expected in the foreground period, normalized by the square root of the variance. The expected number is the number that most likely would occur if the back-

ground rate persisted during the foreground period. Thus, areas with $\beta \geq 3$ (dark red, orange or yellow) may have experienced statistically significant rate increases over the background rate. The color represents the value of the statistic β, which takes on positive values (red, yellow) for rate increases, negative (blue) values for rate decreases. The three dark blue areas apparent in all the color figures (see Figure 2) correspond to the 1990 Upland, 1987 Whittier Narrows and 1989 Malibu aftershock sequences, all of which occurred during the background period. Areas in which there are too few earthquakes to calculate β are white. Because β is derived solely from the numbers of earthquakes in given intervals, it is not sensitive to changes in average earthquake magnitude (b-value) or seismic moment release.

Figures 2-5, 7-8 and 15-16 show β calculated for $M \geq 1.0$ earthquakes. The fact that the catalog is not complete at this magnitude level does not necessarily affect the calculation of β. If the proportion of small events included in the catalog is the same in the background and foreground periods, no first-order effect from working below the completeness threshold would be expected in the calculation of β. However, if the completeness level of earthquake reporting *changes* from the background period to the foreground period, β will reflect the change. The reporting of small events in the southern California catalog changed significantly at the time of the Northridge earthquake, with a smaller percentage of the smaller events being included in the catalog after the earthquake than before (Lucile M. Jones, personal communication). Such an ephemeral recovery period is typical of regional seismograph networks after a large earthquake. This change has an effect on our calculations.

I assume that the only significant change in reporting in the study area between July 1, 1987 and July 17, 1994 is the Northridge-related change just described. There may have been similar recovery periods, during which small events may have been underreported, after the Whittier Narrows, Malibu, Pasadena, Uplands and Landers earthquakes, but these perturbations are not expected to greatly affect the calculation of β because they were transient and short compared to the background period. The post-Northridge artificial deficit of small events in the catalog will tend to pull the colors in Figures 7 and 8 toward blue. For this reason, I refrain from interpreting any blue feature as a post-seismic rate decrease, as it might be an artifact of the reporting change. In addition, the three most significant negative (blue) features in (see Figure 2, for example) are artifacts of a different kind. They correspond to the following aftershock sequences, which, having occurred in the background period, have skewed the calculation of β toward blue in their respective aftershock zones: Whittier Narrows (M 5.9) 1 October, 1987; Malibu (M 5.0) 19 January, 1989; Upland (M 5.4) 28 February, 1990.

With these possible artifacts in mind, I confine my observations to the (red and yellow) areas of apparent seismicity rate increase. In previous work, statistical significance has been associated with values of β greater than about 3, in absolute value. A discussion of significance levels associated with β is given in Matthews and Reasenberg (1988) and Reasenberg and Matthews (1988).

SEISMICITY IN THE YEAR BEFORE THE MAINSHOCK

The average seismicity rate in the study area increased during the half-year period before the Northridge earthquake (Figures 2-5). This trend can be seen as an increasing amount of dark red area, corresponding to increasing values of β, in the sequence comprised of Figures 2-5. During this period, the rate of seismic moment release in the study area also increased (Figure 6). This increase is comparable in magnitude to the quarterly increases and decreases in moment release during the previous year in the same area (Figure 6). The increase in seismic moment in the study area during the 6 months before the Northridge earthquake was produced entirely by $M \geq 3$ earthquakes; release of seismic moment by $1 \leq M < 3$ earthquakes remained essentially constant over this period. The maximum magnitude earthquake increased in each of the four quarters before the Northridge earthquake, but always remained below 4.0, typical for the region.

The quarter-year before the Northridge earthquake included more intense seismicity changes than did the previous 3 quarter-year periods (Figure 5). Areas surrounding the future site of the Northridge earthquake were more active in this period than in the previous 3 quarter-year periods. Activity increased both north of the aftershock zone along the E-W thrust belt north of Ventura basin (roughly in zones J, A and D), and south of the aftershock zone at the northern end of the Palos Verdes fault (zone G). All these areas continued to produce elevated seismicity rates after the Northridge earthquake (Figure 7). The most intense activity in this quarter (in terms of seismic moment release) was in zone G, near Malibu, where 5 ($M \geq 3$) events occurred

between 1 and 8 days before the Northridge earthquake.

SEISMICITY IN THE FIRST 3 MONTHS AFTER THE MAINSHOCK

The aftershock activity was confined to an oblate area approximately 30 km across (yellow area in Figure 7). Outside the aftershock zone, at distances between 20 and 60 km from its center, several smaller, isolated regions experienced elevated seismicity after the mainshock. To the northwest, four clusters of earthquakes (A to D) form a west-trending zone from the San Gabriel fault along the Santa Inez, Arroyo Parida and San Cayetano faults toward Santa Barbara, along the northern edge of the Ventura basin. Since 1987, zones A through D have produced occasional small clusters averaging, together, 33 events ($M \geq 1$) per year. In the first 90 days after the Northridge earthquake 71 earthquakes occurred there - approximately 8 times the background rate. Zones A and J are sites of swarms that began in the summer and fall of 1993 (Figures 4-5). Zones B and C activated after the Northridge earthquake and were seismically quiet during the year before. Zone D activated before the Northridge earthquake (Figure 5), both east and west of the San Gabriel fault, and continued active after the Northridge earthquake on the west side only.

South of the aftershock zone earthquake activity (E) along the Malibu fault, in the Santa Monica Mountains south of Thousand Oaks, began after the Northridge earthquake; the seismicity rate in this area was normal (i.e., not significantly different from the background rate) throughout the year before the earthquake (Figures 2-5). Activity (F) along the Santa Monica fault, near its intersection with the Newport-Inglewood

fault, began after the Northridge earthquake; seismicity there had been normal throughout the previous year. Activity increased in a broad area (G) near the northern ends of the Palos Verdes and Newport-Inglewood faults after the Northridge earthquake. As noted above, a compact, offshore cluster had occurred in the western part of zone G near the Palos Verdes fault one week before the Northridge earthquake (Figure 5).

The post-Northridge earthquake seismicity changes outside the immediate rupture area (Figure 7) include strong rate increases along the Santa Monica-Malibu fault system south of the mainshock and the Arroyo Parida-Santa Inez-San Cayetano fault system to the north. It is perhaps not surprising that increases were roughly confined in these areas; these broad, roughly E-W trending fault systems have been active at least since 1978 (Goter, 1992) while the region between them, including the Ventura basin, Simi and San Fernando valleys, have been relatively quiet since then.

In order to create the images of seismicity rate change shown by color in Figures 2-5 and 7, spatial smoothing was used. The appearance of the resulting images depends to some extent on the smoothing. For example, the rate changes calculated in Figure 7 are recalculcated in Figure 8 using a smaller smoothing kernel. With the smaller smoothing kernel the areas of rate increase in the first quarter-year after the Northridge earthquake appear to be confined to more discrete, isolated and smaller clusters. However, the main features in the spatial distribution of the seismicity rate increases are similar in both figures.

The pattern of rate increases in the 3-month period after the Northridge earthquake revealed by the $M \geq 1.0$ cataloged events (Figure 7) is also apparent in the $M \geq 1.5$ data (Figure 9), and may be qualitatively perceived (but with too few earthquakes to infer statistical significance) in the $M \geq 2.0$ data (Figure 10).

Figures 11 and 12 show cumulative counts of $M \geq 1$ earthquakes in the zones indicated by boxes in Figure 7, starting in 1990 and 1993, respectively. I've placed arrows in Figure 12 to mark possible approximate times of onset of enhanced activity in zones A through E near the time of the Northridge earthquake. The choices of these times were made subjectively; the choice for zone D is the most uncertain, and all of these proposed onset times are tentative, both in their identification as being noteworthy and in their onset times. Zone G began *before* the Northridge earthquake, as noted above. Clusters in zones A, B, C and D began approximately 84, 36, 11 and 0 days, respectively, after the mainshock, in a pattern of apparent outward migration from the San Gabriel fault toward Santa Barbara along the north side of the Ventura Basin. An apparent moveout is seen, with delay time to the onset of post-Northridge activity increasing with distance of the cluster from the center of the aftershock zone (Figure 14). This observation is not supported, however, by the $M \geq 2$ data (Figure 13).

SEISMICITY IN THE SECOND 3-MONTH PERIOD AFTER THE MAINSHOCK

The seismicity rate change index, β, for the second quarter-year period after the

Northridge earthquake (17 April to 17 July) was calculated relative to the same background period used in the previous section (July 1, 1987 to January 17, 1993), and is shown in Figures 15 and 16. The main aftershock zone of the second quarter coincides with the area of intense aftershock activity in the first quarter. Seismicity north of the aftershock zone, just west of the San Gabriel fault, which was high in the first quarter, remained significantly elevated in the second quarter. No migration of activity northward along the San Gabriel fault beyond the extent of the first quarter activity has occurred.

Parts of the E-W trending belt of activity north of the Ventura basin that were active in the first quarter remained so in the second quarter, while other parts decreased in activity. Activity on the Santa Inez fault subsided in the second quarter, but activity along the Arroyo Parida and San Gabriel faults persisted. If the clusters of seismicity in this broad, roughly E-W trending thrust belt can be considered together, they form a perforated line of seismicity extending from the San Gabriel fault some 80 km west to just offshore near Santa Barbara. Activity on this belt decreased close to the aftershock zone (north of Simi Valley) and continued active farther west (near zone J), toward the coast near Santa Barbara.

South of the aftershock zone relatively high levels of seismicity persisted along the northern stretches of the Newport-Inglewood and Palos Verdes faults. The activity in the first quarter along the Malibu fault subsided in the second quarter. New clusters of activity have occurred in the second quarter farther southeast along the Newport-Inglewood fault, near Long Beach and Huntington Beach.

Seismicity near the intersection of the San Andreas and Garlock faults increased during the second quarter and spread north. During the first quarter, there was a small cluster of seismicity near this location, just south of the San Andreas fault near the town of Gorman. Seismicity in this area increased in the second quarter and extended north of the San Andreas fault, toward the town of Grapevine.

On the Mojave segment of the San Andreas fault 3 earthquakes were located during the second quarter, near Pearblossom and near the location of the sole event recorded near this segment of the San Andreas during the first quarter. This activity level is too low to indicate anything about the hazard state of the San Andreas here, or its change in stress.

SUMMARY AND CONCLUSION

During the half-year period before the Northridge earthquake, seismicity increased in the study area. This increase was concentrated in clusters north of the Ventura basin, near the San Gabriel fault, and near the intersection of the Malibu and Palos Verdes faults. The average seismic activity in the study area during this half-year period was relatively high, but was not at unprecedented high levels of activity for this area.

During the first 3-month period after the Northridge earthquake, intense aftershock activity occurred within approximately 20 km distance from the mainshock epicenter. Beyond that distance, earthquake activity increased in clusters near the San Gregorio fault and along the northern edge of the Ventura basin. These clusters form a

west-trending belt that roughly coincides with a zone of increased activity during the half-year period before the earthquake. During the first quarter-year period after the Northridge earthquake, seismic activity also increased in areas south of the aftershock zone, near the Malibu fault and near the intersection of the Santa Monica and Newport-Inglewood faults. The Mojave segment of the San Andreas fault was quiet.

During the next 3 months (April 17 to July 17, 1994), elevated levels of seismic activity continued in areas north of Ventura basin, near the San Gregorio fault, and south of the Santa Monica fault, near the Newport-Inglewood fault. New areas of clustered activity began farther south, east of the Newport-Inglewood fault, near Long Beach and Huntington Beach. Seismicity near the Malibu fault subsided. Seismicity near the intersection of the San Andreas and Garlock faults increased. The Mojave segment of the San Andreas fault remained quiet.

The spatial and temporal patterns of elevated seismic activity before and after the Northridge earthquake may be related to processes leading up to the Northridge earthquake. For example, we may ask the following hypothetical questions. Did a regional strain event trigger *both* the 6-month pre-earthquake pattern of increased seismicity *and* the Northridge earthquake itself? The similarity in the patterns of pre- and post-earthquake seismicity outside the immediate aftershock zone might suggest this. Is the extended pattern of elevated seismicity north of the Ventura basin after the Northridge earthquake indicative of a future large earthquake west of the Northridge earthquake? Are the areas of elevated seismicity in the half-year before the Northridge earthquake seismic "sensitive spots" that registered a regional strain or weakening in this part of

southern California? If so, will they do so next time? Alternatively, we must consider the possibility that the observed patterns in seismicity are simply "noise" unrelated (in a predictive sense) to the Northridge earthquake and to future large earthquakes in the region. In this preliminary report, we stop short of constructing a tectonic interpretation of the seismicity patterns presented here for two reasons. First, while we are free to speculate and hypothesize, we know of no dependable guidelines for the interpretation of the seismicity patterns before large earthquakes, a point that was emphasized in the Introduction. In the area of interpreting seismicity patterns, we are very much still in the learning phase. In addition, the particular arrangement of active faults in the study area, the contemporary displacement rates on them and the regional deformation are just now becoming known or modeled as a result of numerous geologic and geophysical investigations launched or accelerated after the Northridge earthquake. As these results more fully emerge, perhaps the seismicity patterns will begin to make more sense. At this time, we offer the seismicity observations, *sans* interpretation, as food for thought.

REFERENCES

Agnew, D. C. and L. M. Jones, 1991, Prediction probabilities from foreshocks, J. Geophys. Res., 96, 11,959-11,971.

Goter, S. K., 1992, Southern California Earthquakes (Map), U.S. Geological Survey Open-File Report 92-533.

Harris, R. A., Simpson, R. W., Reasenberg, P. A., (1995), Influence of static stress changes on earthquake locations in southern California, Nature, 375, 221-224.

Healy, J. H., Kossobokov, V. G., Dewey, J. W., 1992, A test to evaluate the earthquake prediction algorithm, M8, U.S. Geological Survey Open-File Report 92-401.

Hudnut, K. W., Murray, M. H., Donnellan, A., Bock, Y., Fang, P., Hager, B., Herring, T., King, R., 1994, Coseismic displacements of the 1994 Northridge, California, earthquake, Abstracts of the 89th meeting of the Seism. Soc. Am.

Jennings, C.W., 1992, Preliminary fault activity map of California, Calif. Dept. of Conserv. Div. of Mines and Geol. O.F. Rep. 92-03.

Jones, L. M., 1985, Foreshocks and time-dependent earthquake hazard assessment in southern California, B.S.S.A., 75, 1669-1679.

Keilis-Borok, B. I., Kossobokov, V. G., 1990, Times of increased probability of strong earthquakes (M>7.5) diagnosed by algorithm M8 in Japan and adjacent territories, J. Geophys. Research 95, 12413-12422.

King, G. C. P., R. S. Stein, J. Lin, 1994, Static stress changes and the triggering of earthquakes, B.S.S.A. 84, 935-953.

Matthews, M. V., Reasenberg, P. A., 1988, Statistical Methods for Investigating Quiescence and other Temporal Seismicity Patterns, Pure and Applied Geophysics, 126.

Reasenberg, P. A. and L. M. Jones, 1989, Earthquake hazard after a mainshock in California, Science, 243, 1173-1176.

Reasenberg, P. A. and L. M. Jones, 1994, Earthquake Aftershocks: Update, Science, 265, 1251-1252.

Reasenberg, P. A., M. V. Matthews, 1988, Precursory Seismic Quiescence: A Preliminary Assessment of the Hypothesis, Pure and Applied Geophysics, 126.

Reasenberg, P. A., R. W. Simpson, 1992, Response of regional seismicity to the static stress changes produced by the Loma Prieta earthquake, Science, 255, 1687-1690.

Richter, C. R., 1958, Elementary Seismology, W. H. Freeman and Co., San Francisco.

Scientists of the U.S. Geological Survey and the Southern California Earthquake Center, 1994, The magnitude 6.7 Northridge, California, earthquake of January 17, 1994, Science, 266, 389-397.

Stein, R. S., G. C. P. King, J. Lin, 1994, Stress triggering of the 1994 M=6.7 Northridge, California earthquake by its predecessors, Science, 265, 1432-1435.

Stein, R. S., G. C. P. King, J. Lin, 1992, Change in failure stress on the southern San Andreas fault system caused bythe 1992 M=7.4 Landers earthquake, Nature, 258, 1432-1435.

Sykes, L. R., Jaume, S. C., 1990, Seismic activity on neighbouring faults as a long-term precursor to large earthquakes in the San Francisco Bay area, Nature, 348,

595-599.

FIGURE CAPTIONS

Figure 1. Active faults (Jennings, 1992) in the southern California region surrounding the January 17, 1994 Northridge earthquake. AP = Arroyo Parida fault; BP = Big Pine fault; GF = Garlock fault; M = Malibu fault; NI = Newport-Inglewood fault; OR = Oak Ridge fault; PM = Pine Mountain fault; PV = Palos Verdes fault; S = Simi fault; SC = San Cayatano fault; SG = San Gabriel fault; SM = Sierra Madre fault; SMA = Santa Monica fault; SS = Santa Suzanna fault; W = Whittier fault. Rectangle represents the surface projection of the south-dipping, 8 km long by 10 km tall model fault plane for the Northridge earthquake inferred from geodetic observations by Hudnut et al. (1994).

Figures 2-5. Visualization of seismicity changes. Seismicity in each of four consecutive, non-overlapping 3-month intervals before the Northridge earthquake is compared to the seismicity in a fixed background period July 1, 1987 to Jan 17, 1993. The three-month intervals are specified at the top of each figure. Earthquakes ($M \geq 1$) in each 3-month period are plotted as black circles. Color represents values of the seismicity rate index β, which is a measure of the rate change in the 3-month period, relative to the background period. Positive values of β (red, orange, yellow) represent seismicity rate increases in the 3-month interval relative to the background rate. Negative values of β (blue) represent decreases in rate, relative to the background rate. Active faults, taken from Jennings (1992), are shown as solid black lines. Three dark blue areas annotated in Figure 2 correspond to aftershock sequences in the background period: A = Whittier Narrows (M 5.9) 1

October, 1987; B = Malibu (M 5.0) 19 January, 1989; C = Upland (M 5.4) 28 February, 1990

Figure 6. Seismic moment release corresponding to ($M \geq 1.0$) earthquakes in the study area in consecutive, non-overlapping 3-month intervals two years before and 6 months after the Northridge earthquake. Heights of the dark gray, light gray and black portions of each bar correspond to the total seismic moment released by earthquakes with $1 \leq M < 2$, $2 \leq M < 3$ and $M \geq 3$, respectively. Maximum magnitude of earthquakes in each 3-month period are shown on top of bars.

Figure 7. Same as Figures 2-5, except that the the test interval is the first 3-month period after the Northridge earthquake (January 17 to April 17, 1994). The Northridge aftershock zone is the black mass of earthquakes underlain by yellow. Zones of seismicity outside the aftershock zone, defined by the prominant clusters of earthquakes in this period, are shown by boxes A through L. Prominant clusters of earthquakes north of the aftershock zone suggest a west-trending band from the San Gregorio fault to the northern edge of the Ventura basin. Prominant clusters also occurred south of the aftershock zone, near the Malibu, Santa Monica and Palos Verdes faults.

Figure 8. Same as Figure 7, except spatial smoothing used to produce the color image employed a 2-km-radius gaussian smoothing kernel, rather than the 5-km-radius smoothing kernel used in Figures 2-5 and Figure 7 (see text).

Figure 9. Same as Figure 7, but for earthquakes with $M \geq 1.5$. The pattern of post-Northridge earthquake activity apparent in Figure 7 is still apparent here.

Figure 10. Same as Figure 7, but for earthquakes with $M \geq 2.0$. The spatial pattern of post-Northridge earthquake activity apparent in Figures 7 and 9 is barely visible in this reduced data set.

Figure 11. Cumulative number of $M \geq 1$ earthquakes in each zone defined by boxes in Figure 7, during the period January 1, 1990 to July 17, 1994. Number printed below each zone name is the total number of events in the plot. Vertical lines mark the times of the Landers, California (June 28, 1992; M 7.3) earthquake, the Northridge earthquake and the date April 17, 1994 (3 months after the Northridge earthquake).

Figure 12. Same as Figure 11, but for the period beginning Jan 1, 1993. Arrows indicate my estimates of the apparent times of onset of increased seismic activity near the time of the Northridge earthquake in zones A through E. Vertical lines mark the times of the Northridge earthquake and the date April 17, 1994 (3 months after the Northridge earthquake).

Figure 13. Same as Figure 11, but for $M \geq 2$ earthquakes only.

Figure 14. Plot of time of onset of prominent clusters of post-Northridge activity, relative to the mainshock, in selected zones versus approximate distance of the cluster to the center of the Northridge aftershock zone. An apparent migration of activity outward from the aftershock zone may have decreased in velocity from about 1 km/day during the first two weeks after the Northridge earthquake to about 0.2 km/day two months later.

Figure 15. Seismicity in the second 3-month period after the mainshock (17 April to 17 July, 1994). Background period used for reference in calculating seismicity rate changes and all other conditions are as specified in the caption for in Figure 7.

Figure 16. Same as Figure 15, except spatial smoothing used to produce the color image employed a 2-km-radius gaussian smoothing kernel rather than the 5-km-radius smoothing kernel used in Figure 15 (see text).

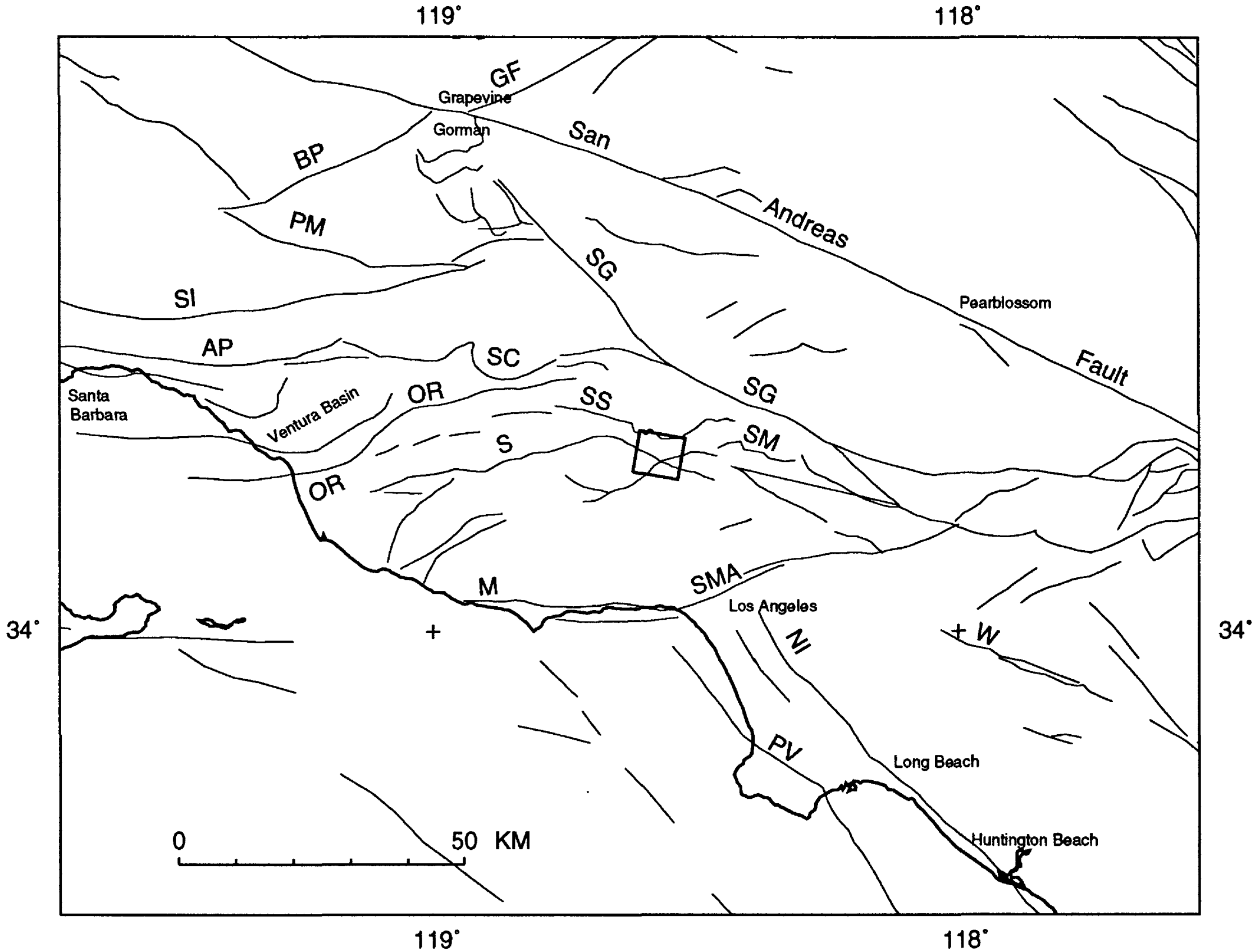

Mon Sep 19 10:06:30 1994
OF_fig1.ans

Fig. 1

Jan 17 '93 - Apr 17 '93

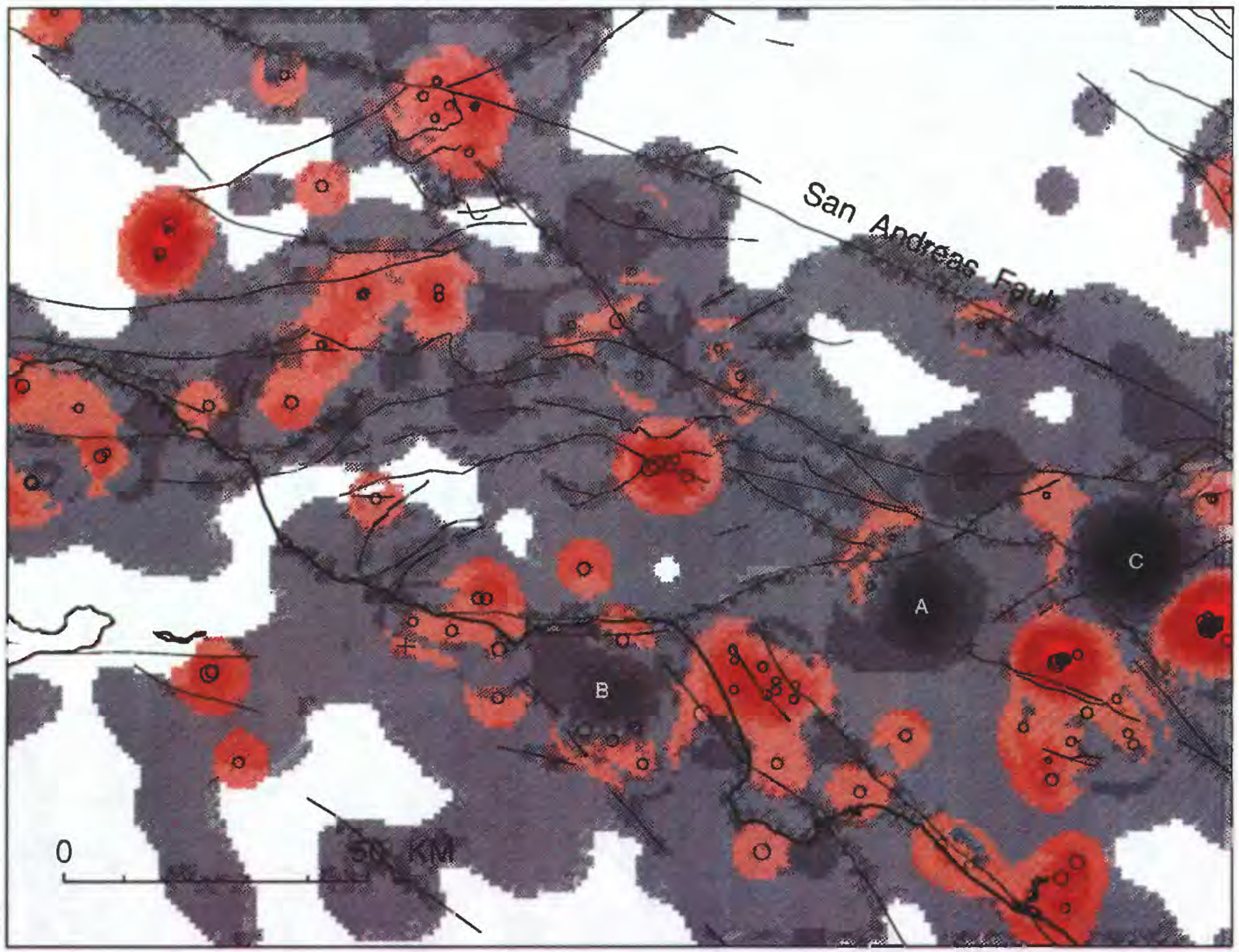

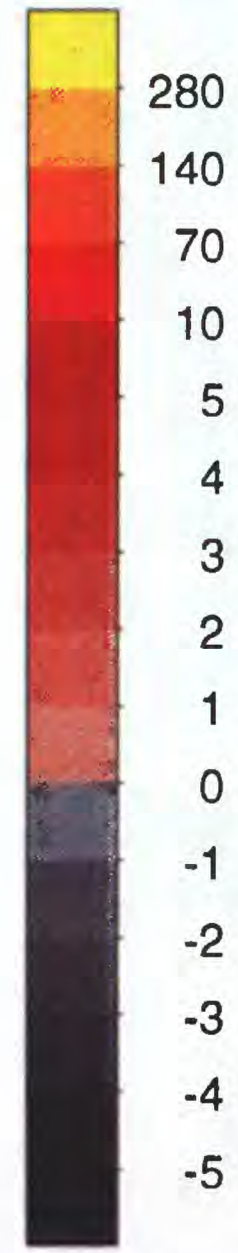

25

Seismicity Rate Changes

Comparison of 870701-930117 to 930117-930417 (M>1)
Red/Yellow = Increase in Rate Relative to Background

Wed Sep 21 11:04:41 1994
OF_fig2.ans

Fig. 2

Apr 17 '93 - Jul 17 '93

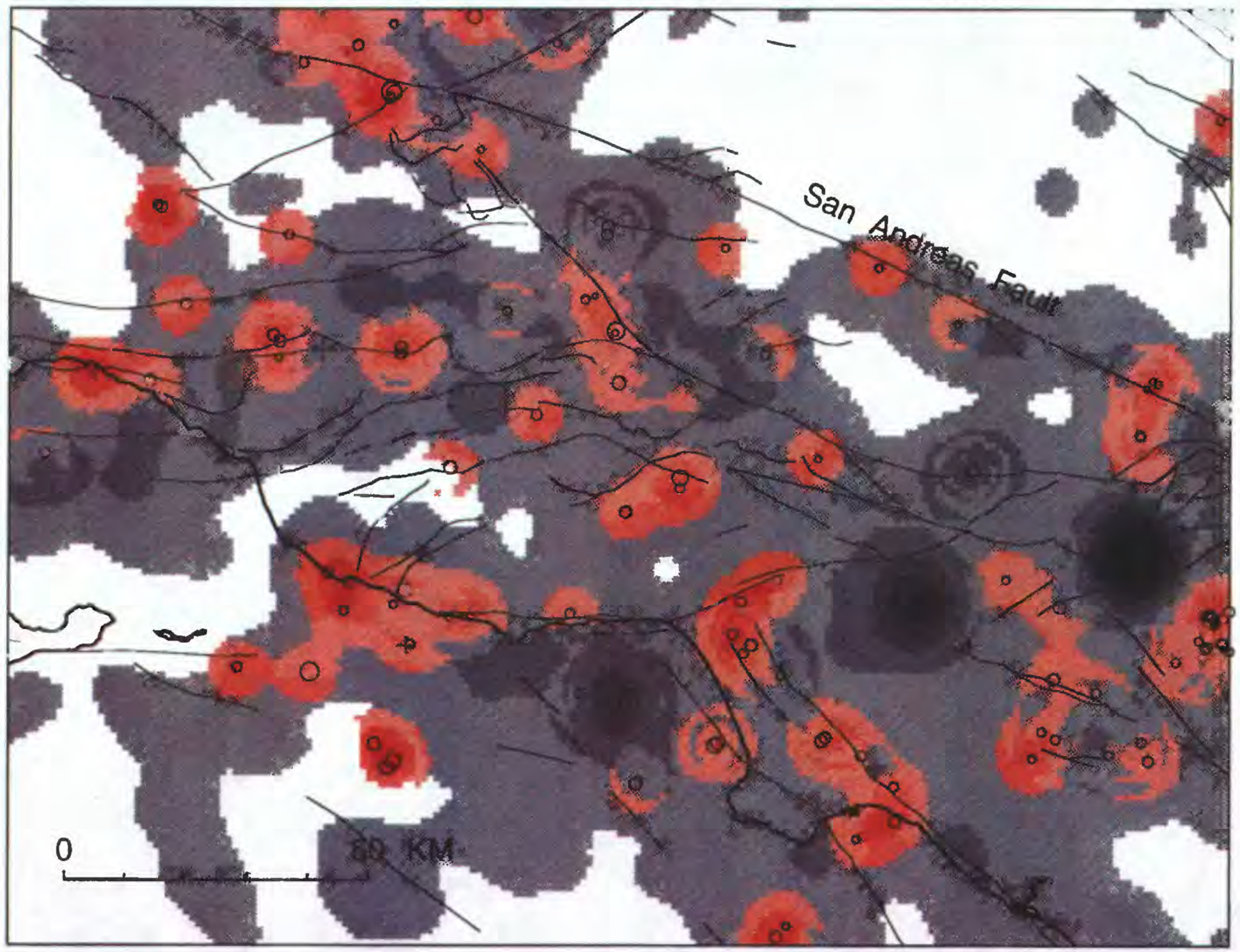

BETA

280
140
70
10
5
4
3
2
1
0
-1
-2
-3
-4
-5

92

Seismicity Rate Changes

Comparison of 870701-930117 to 930417-930717 (M>1)
Red/Yellow = Increase in Rate Relative to Background

Wed Sep 21 11:06:47 1994
OF_fig3.ans

Fig. 3

Jul 17 '93 - Oct 17 '93

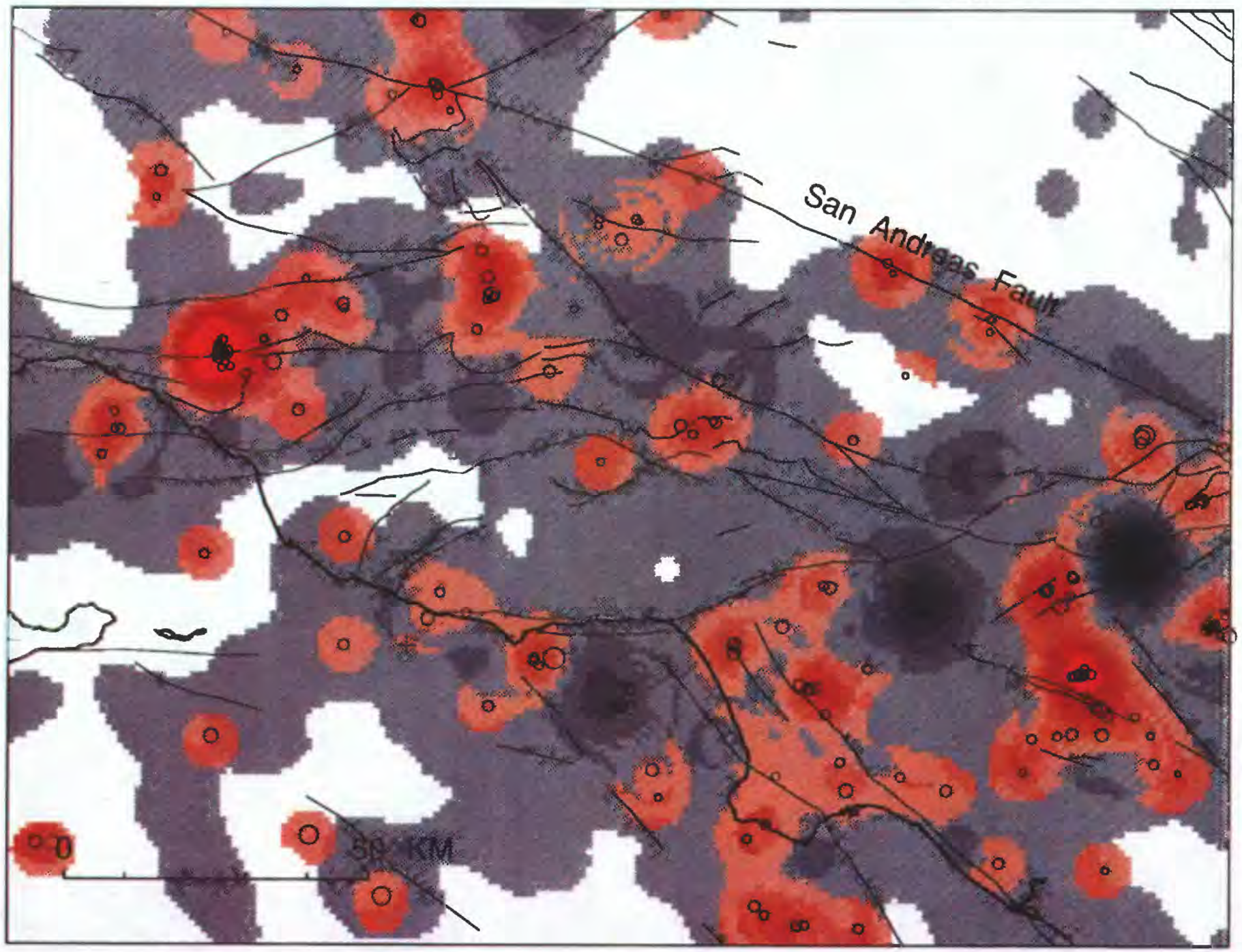

27

Seismicity Rate Changes

Comparison of 870701-930117 to 930717-931017 (M>1)
Red/Yellow = Increase in Rate Relative to Background

Wed Sep 21 11:07:50 1994
OF_fig4.ans

Fig. 4

Oct 17 '93 - Jan 17 '94

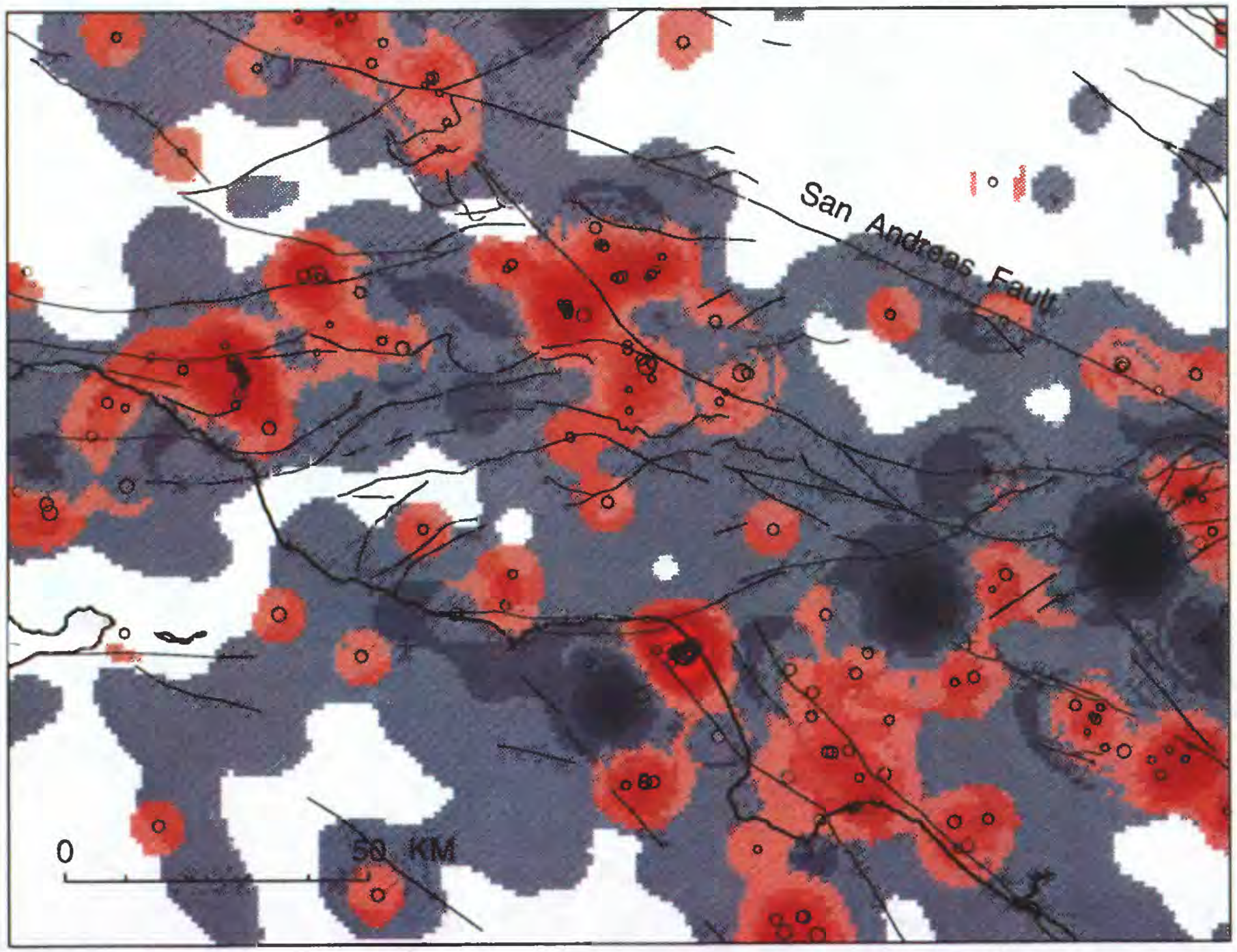

28

Seismicity Rate Changes

Comparison of 870701-930117 to 931017-940117 (M>1)
Red/Yellow = Increase in Rate Relative to Background

Wed Sep 21 11:08:49 1994
OF_fig5.ans

Fig. 5

Fig. 6

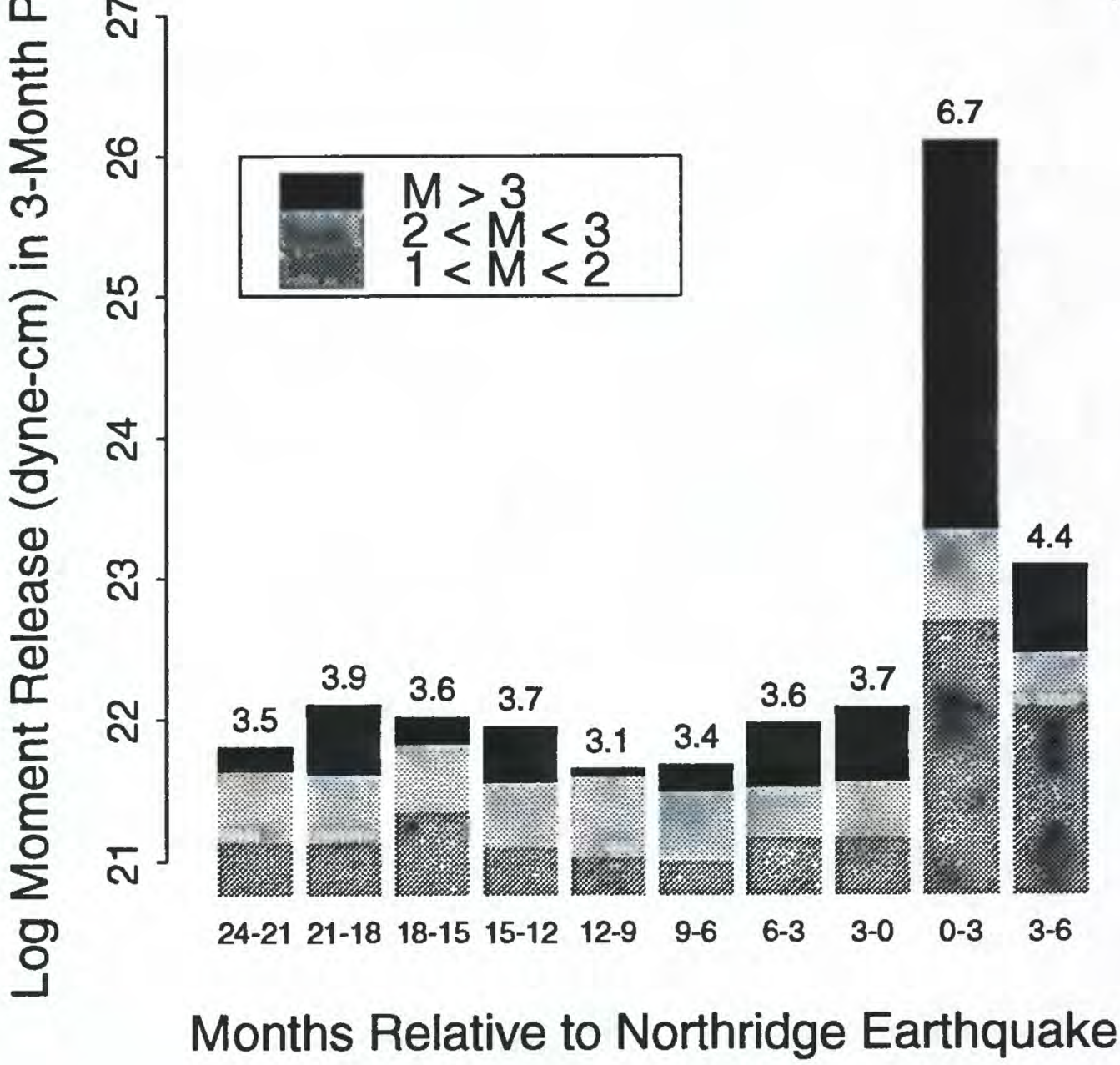
Log Moment Release (dyne-cm) in 3-Month Period
21
22
23
24
25
26
27
M > 3
2 < M < 3
1 < M < 2
3.5
3.9
3.6
3.7
3.1
3.4
3.6
3.7
6.7
4.4
24-21
21-18
18-15
15-12
12-9
9-6
6-3
3-0
0-3
3-6
Months Relative to Northridge Earthquake

Jan 17 '94 - Apr 17 '94

119° 118°

34°

San Andreas Fault

A B C D E F G H J K L

0 50 KM

BETA

280
140
70
10
5
4
3
2
1
0
-1
-2
-3
-4
-5

Seismicity Rate Changes

Comparison of 870701-930117 to 940117-940417 (M>1)
Red/Yellow = Increase in Rate Relative to Background

Wed Sep 21 11:24:17 1994
OF_fig7.ans

Fig. 7

Jan 17 '94 - Apr 17 '94 (2-km smoothing)

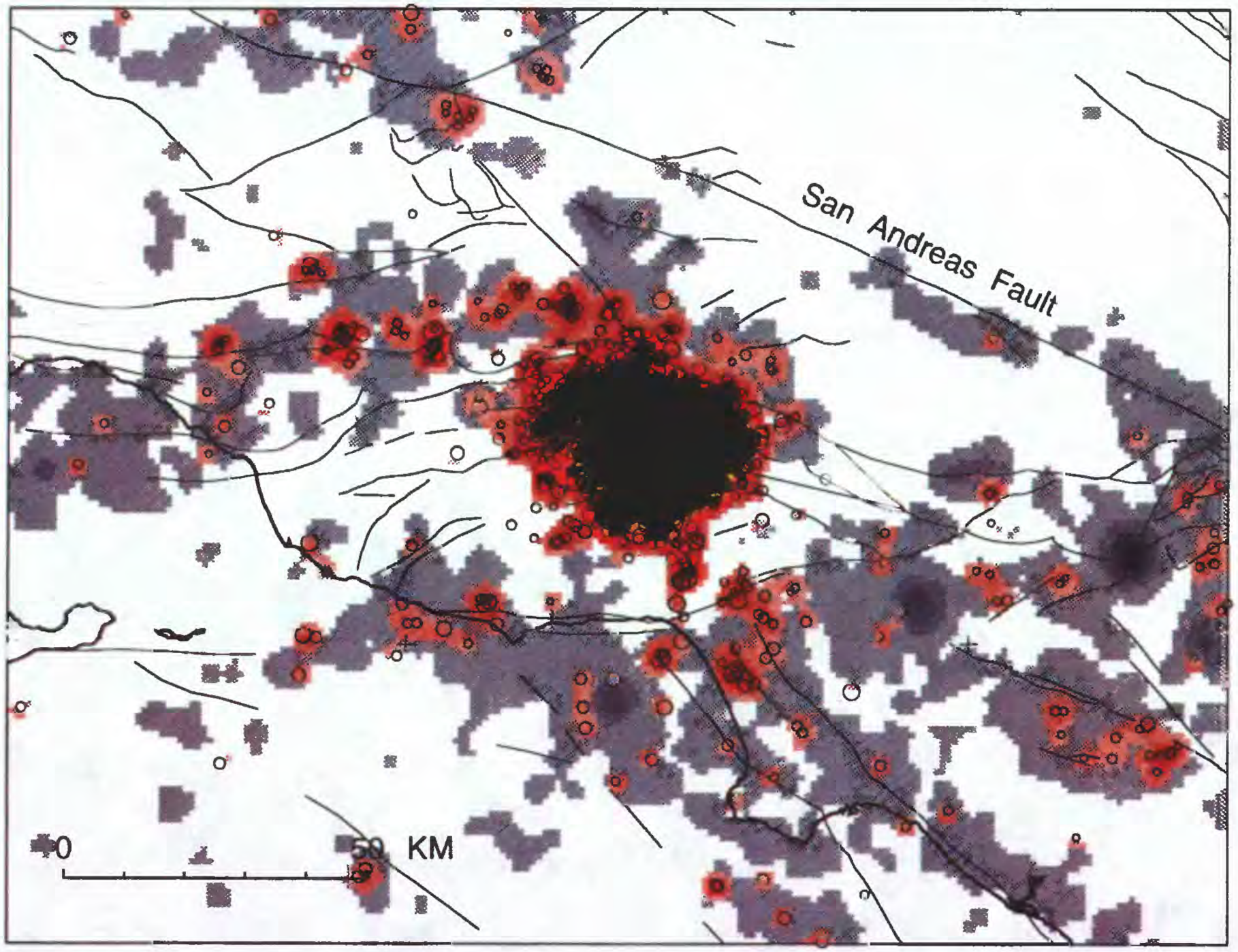

Seismicity Rate Changes

Comparison of 870701-930117 to 940117-940417 (M>1)
Red/Yellow = Increase in Rate Relative to Background

Wed Sep 21 11:26:03 1994
OF_fig8.ans

Fig. 8

Jan 17 '94 - Apr 17 '94 (M > 1.5)

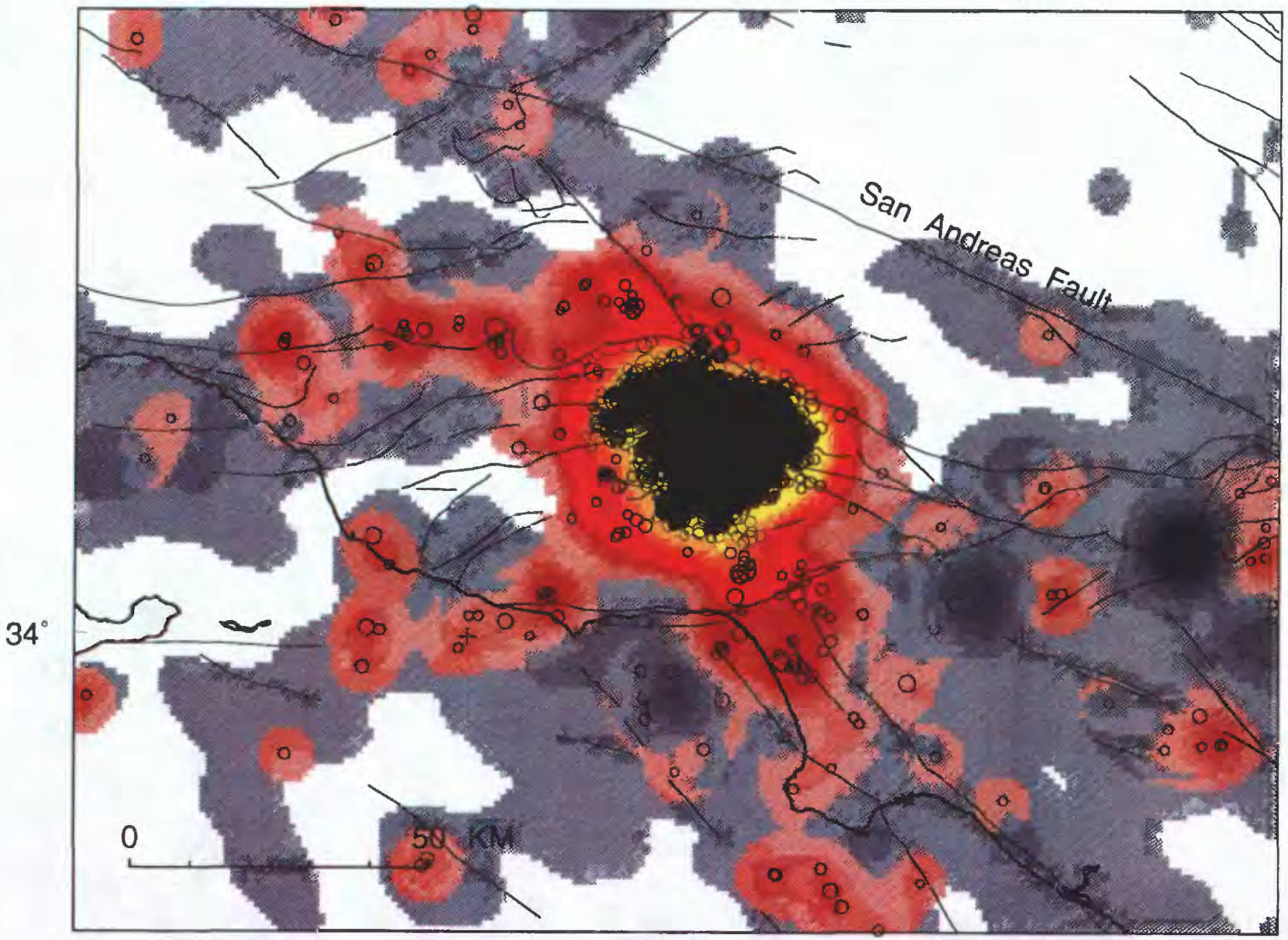

32

Seismicity Rate Changes

Comparison of 870701-930117 to 940117-940417 (M>1.5)
Red/Yellow = Increase in Rate Relative to Background

Wed Sep 21 11:27:44 1994
OF_fig9.ans

Fig. 9

Jan 17 '94 - Apr 17 '94 (M > 2.0)

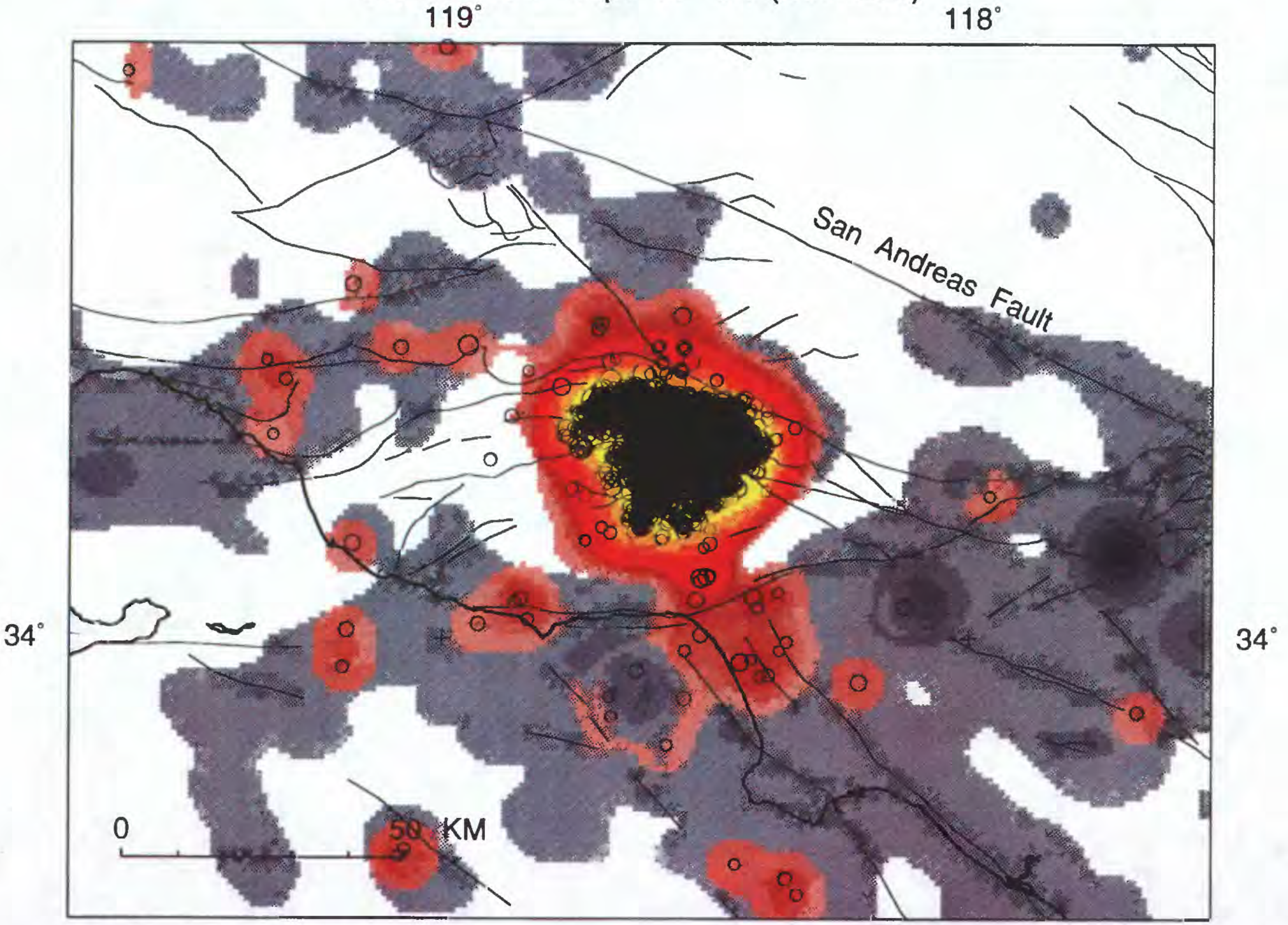

Seismicity Rate Changes

Comparison of 870701-930117 to 940117-940417 (M>2)
Red/Yellow = Increase in Rate Relative to Background

Wed Sep 21 11:29:10 1994
OF_fig10.ans

Fig. 10

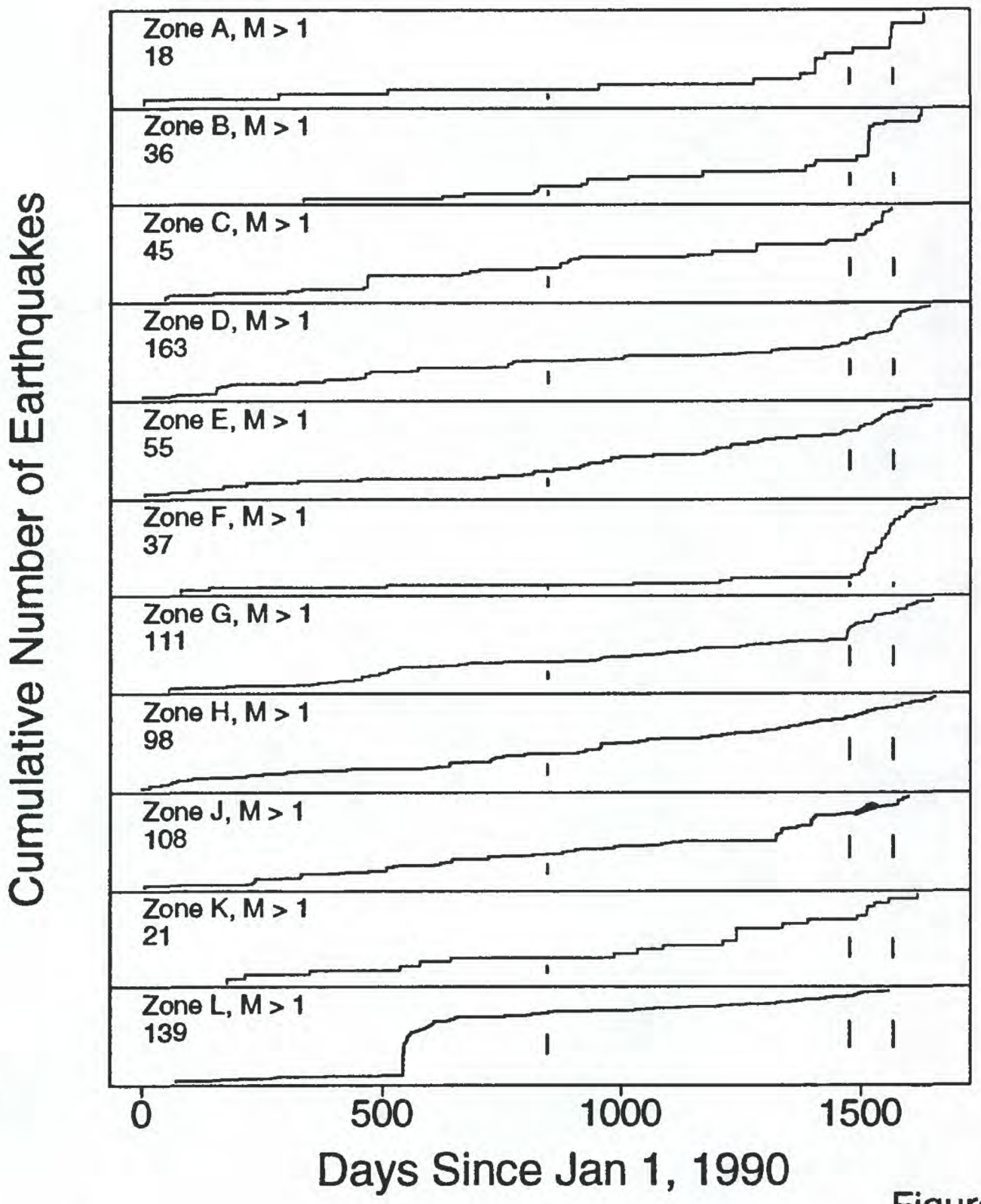
Zone A, M > 1
18
Zone B, M > 1
36
Zone C, M > 1
45
Zone D, M > 1
163
Zone E, M > 1
55
Zone F, M > 1
37
Zone G, M > 1
111
Zone H, M > 1
98
Zone J, M > 1
108
Zone K, M > 1
21
Zone L, M > 1
139
Cumulative Number of Earthquakes
0
500
1000
1500
Days Since Jan 1, 1990

Figure 11

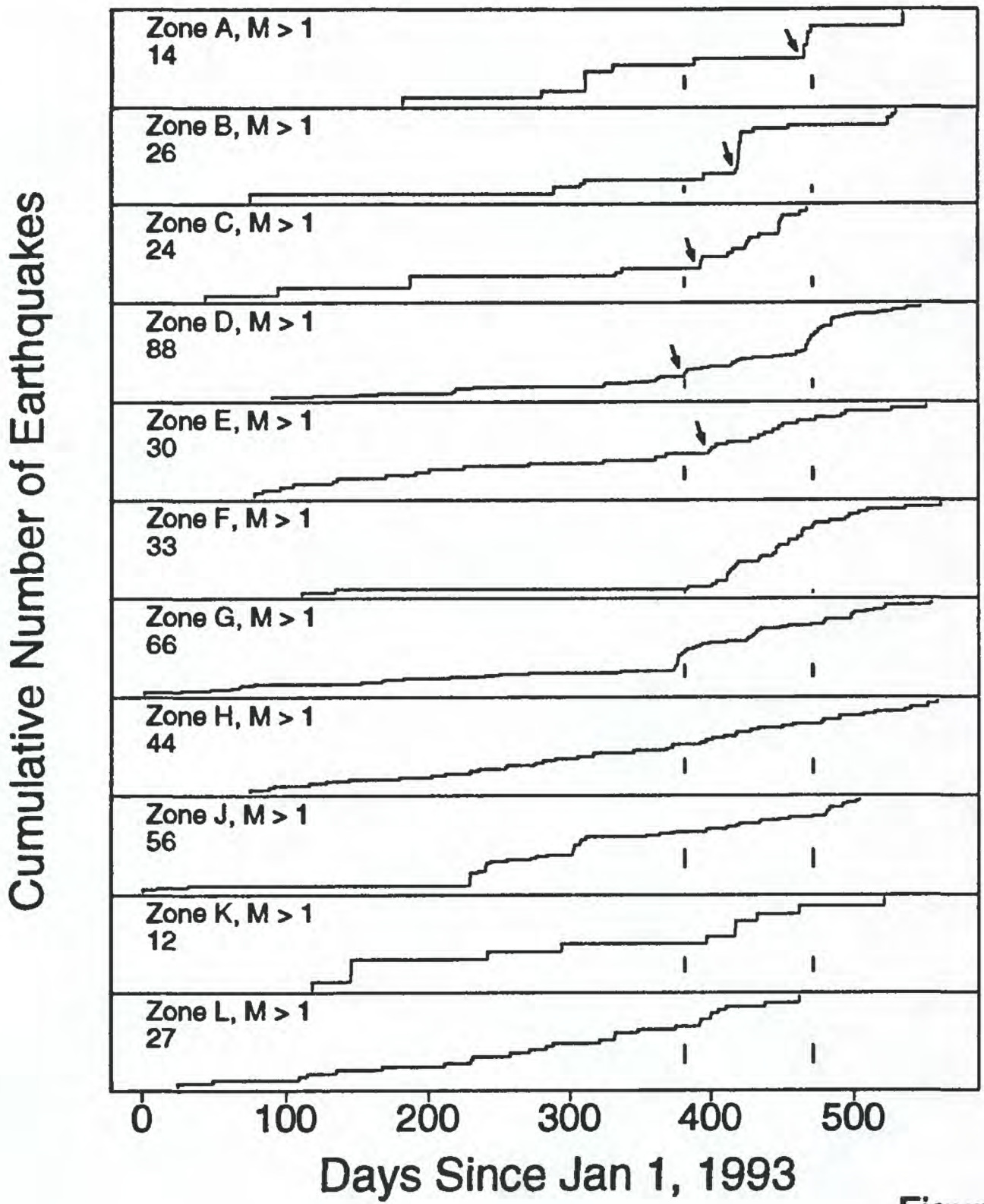
Zone A, M > 1
14
Zone B, M > 1
26
Zone C, M > 1
24
Zone D, M > 1
88
Zone E, M > 1
30
Zone F, M > 1
33
Zone G, M > 1
66
Zone H, M > 1
44
Zone J, M > 1
56
Zone K, M > 1
12
Zone L, M > 1
27
Cumulative Number of Earthquakes
0
100
200
300
400
500
Days Since Jan 1, 1993

Figure 12

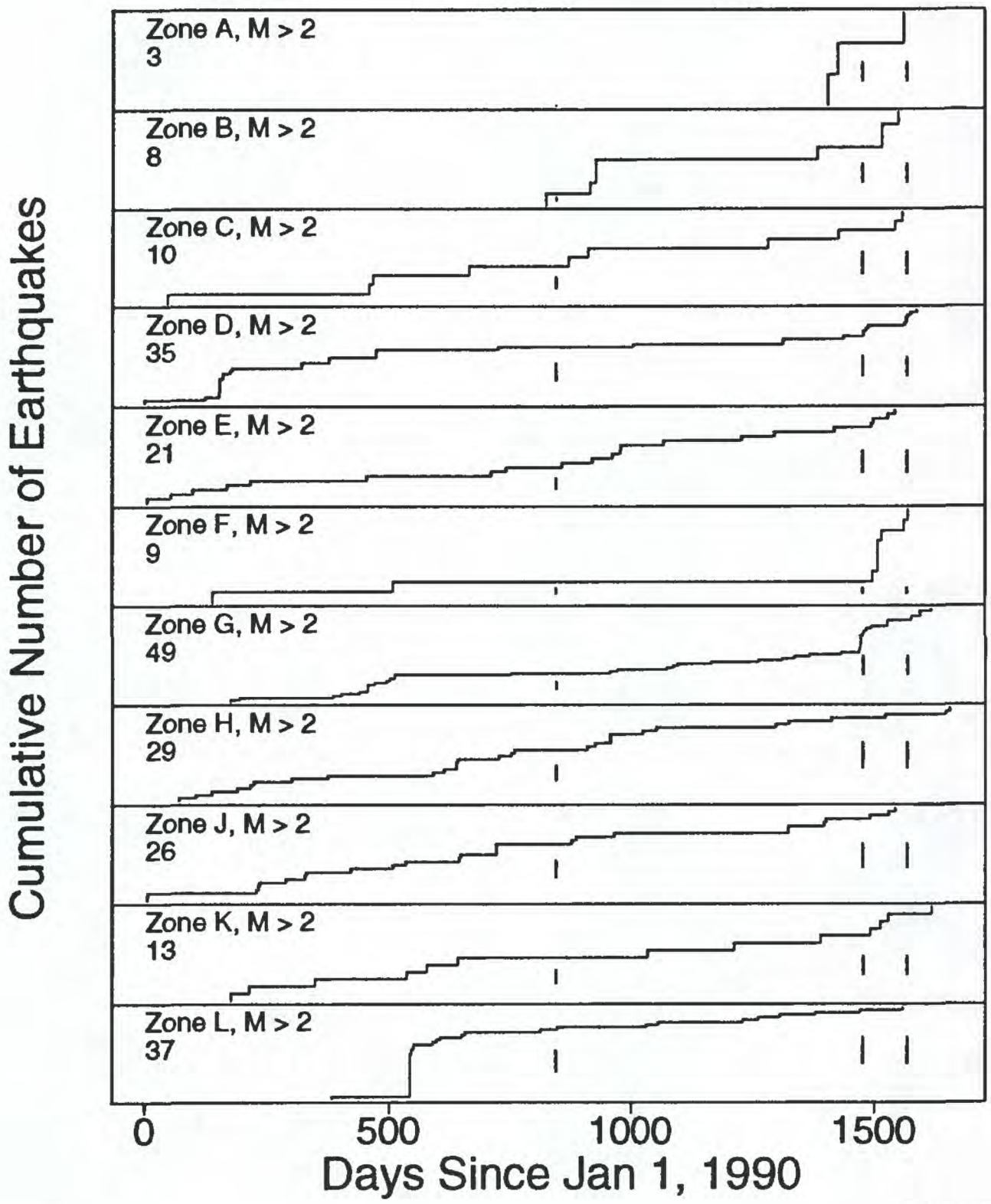
Zone A, M > 2
3
Zone B, M > 2
8
Zone C, M > 2
10
Zone D, M > 2
35
Zone E, M > 2
21
Zone F, M > 2
9
Zone G, M > 2
49
Zone H, M > 2
29
Zone J, M > 2
26
Zone K, M > 2
13
Zone L, M > 2
37
Cumulative Number of Earthquakes
0
500
1000
1500
Days Since Jan 1, 1990

Figure 13

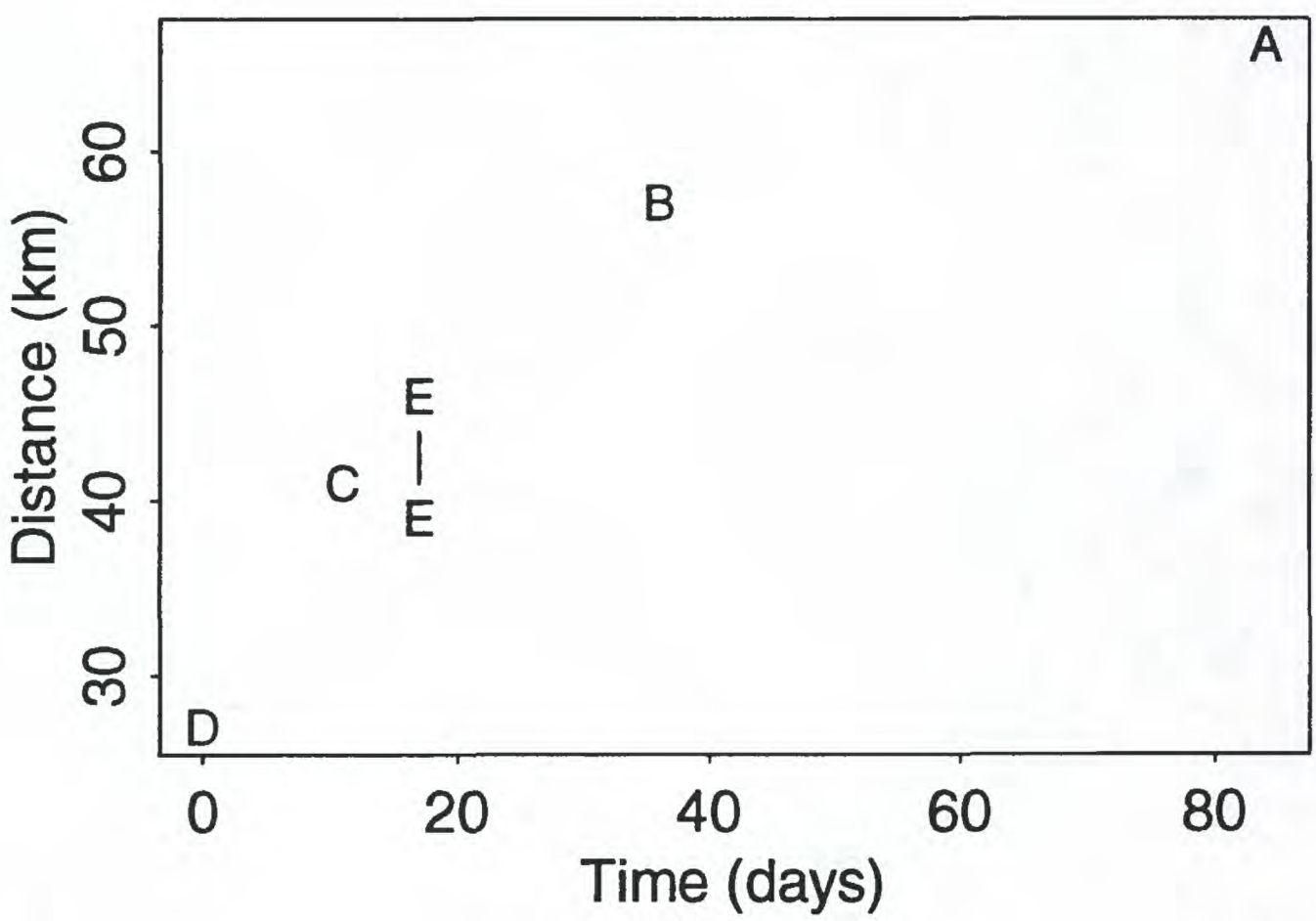

Figure 14

Apr 17 '94 - Jul 17 '94

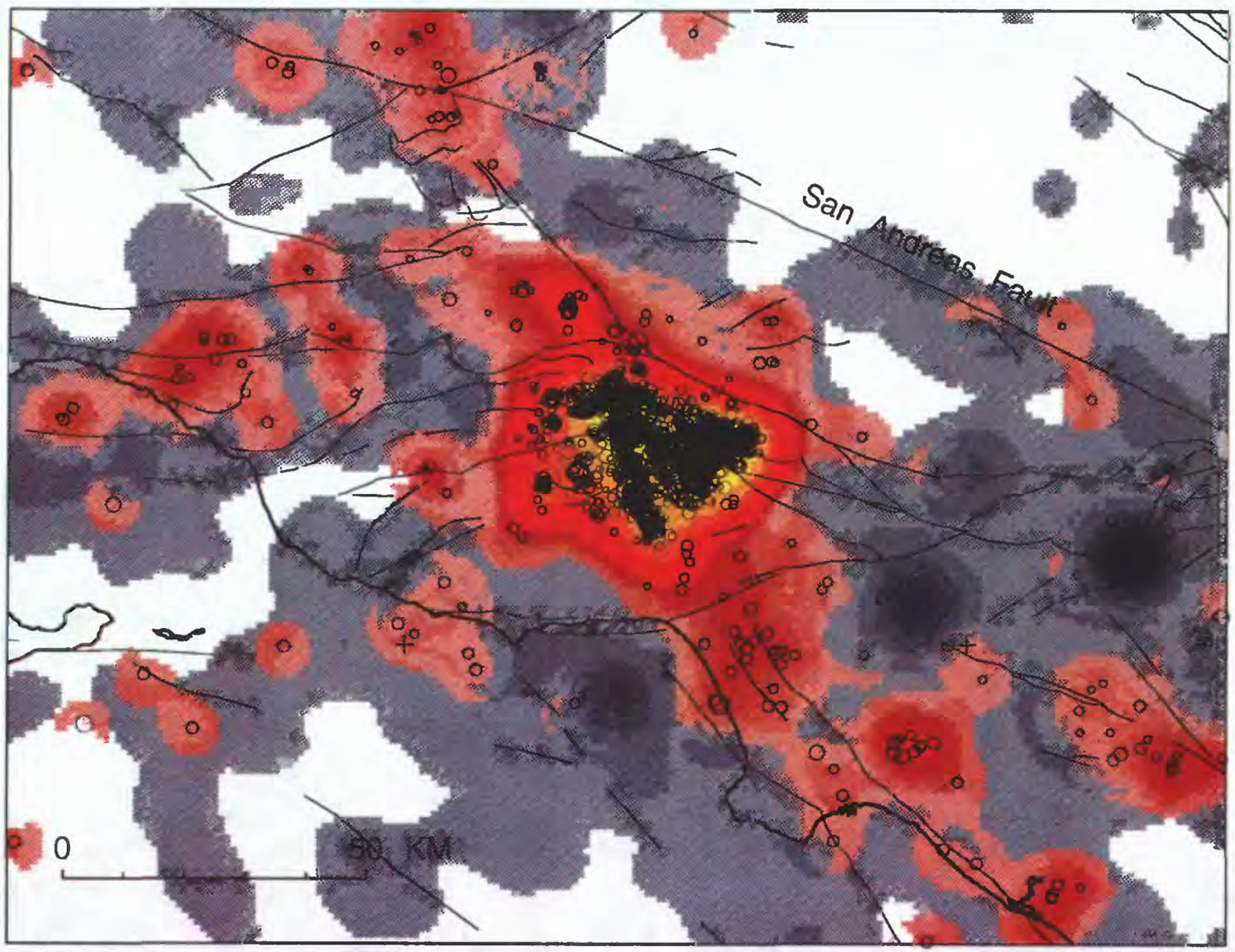

38

Seismicity Rate Changes

Comparison of 870701-930117 to 940417-940717 (M>1)
Red/Yellow = Increase in Rate Relative to Background

Wed Sep 21 11:30:17 1994
OF_fig15.ans

Fig. 15

Apr 17 '94 - Jul 17 '94 (2-km smoothing)

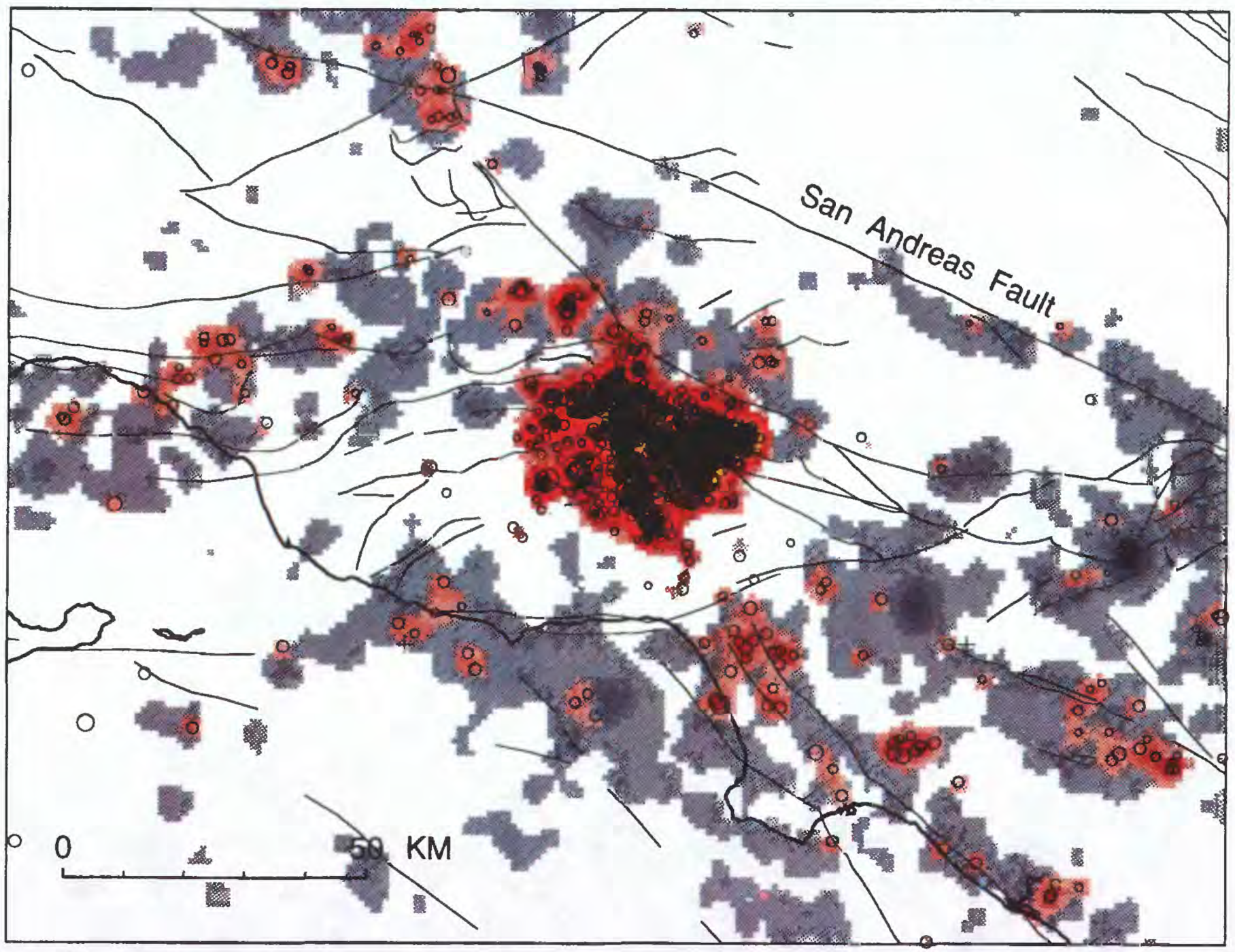

Seismicity Rate Changes

Comparison of 870701-930117 to 940417-940717 (M>1)

Red/Yellow = Increase in Rate Relative to Background

Wed Sep 21 11:31:39 1994
OF_fig16.ans

Fig. 16